A low-cost dual bandpass planar filter for WiMAX and mobile communications

Amal Kadiri[1], Abdelali Tajmouati[1], Jamal Zbitou[2,3], Ahmed Lakhssassi[4]
[1]Mecanic, Informatic, Electronic and Telecommunication Laboratory (MIET), Faculty of Science and Technology, Hassan First University, Settat, Morocco
[2]The Information and Communication Technologies Laboratory (LABTIC), ENSA of Tangier, University of Abdelmalek Essaadi, Tetouan, Morocco
[3]ENSA of Tetouan, University of Abdelmalek Essaadi, Tetouan, Morocco
[4]Laboratory of advanced microsystems engineering, University of Quebec in Outaouais, Gatineau, Canada

Article Info

ABSTRACT

This study proposes a new design of low-cost dual-bandpass filter for worldwide interoperability and microwave access (WiMAX) band at 3.50 GHz and mobile communications band at 1.19 GHz. A high pass filter and a stopband filter make up the new dual-bandpass filter structure. Different theoretical studies were carried out for the design of the proposed filter. This filter's base is a RO5880 substrate with a dielectric permittivity constant of 2.2, loss tangent of 0.0009 and 1.6 mm thickness. High mashing density was used to validate the various simulated structures while accounting for two numerical methods: the moment technique and the finite integration method. The final circuit's overall dimensions are $60 \times 178,3$ mm^2.

Corresponding Author:

Amal Kadiri
Mecanic, Informatic, Electronic and Telecommunications Laboratory (MIET)
Faculty of Science and Technology, Hassan First University of Settat
Settat, Morocco
Email: a.kadiri@uhp.ac.ma

1. INTRODUCTION

The use of mobile devices and telecommunications systems has expanded significantly in recent years. These systems have already seen widespread use in industry, business, housing, and the military. However, the most important factors in the context of an industrial process for equipment supporting radiofrequency devices are streamlining design and manufacture, cutting manufacturing costs, and increasing the equipment's performance. To ensure flawless and accurate transmission and/or reception, this presupposes the application and implementation of strategies for optimizing, miniaturizing, and enhancing the microwave circuits that make up these systems [1]−[8]. This work focuses on the design of a new dual band-pass filter employing planar technology in this context.

Multiband filters are an essential circuit block in multiband wireless communication systems that was recently designed and widely used [9]−[15]. Multiband bandpass filters have garnered a lot of consumer interest as a result of the development and proliferation of multiservice wireless communication systems in a single device. Single-band filters were employed in the past and could only function in one frequency band. Dual band or multi band microwave filters that can be integrated in a single device are required to satisfy user needs. Multiband filters are an essential circuit block in multiband wireless communication systems that

was recently designed and widely used. Several band passes due to their specific characteristics, which means a high selectivity, deep transmission zeros, wide rejection band, an abrupt roll-off rate, and tunable conduct, filters have a special place in radio frequency (RF) receivers. This is especially true given the speed at which wireless communication systems are developing [16]–[18]. Band pass filters are used in a wide range of wireless communication systems, particularly microwave systems with limited space for microwave components and circuits [19]–[23]. The following requirements must be met by this type of filter in order to work with contemporary communication systems: insertion loss reduction in the band, high selectivity, size compactness, and harmonics suppression [24]–[26].

2. METHOD
2.1. Optimum distributed high pass filter

Figure 1 present the design of the distributed highpass filter; Figure 1(a) presents the optimum design and Figure 1(b) presents the fundamental design. It consists of a series of electrically lengthened shunt short-circuited stubs c spaced apart by connecting lines (unit elements) of electrical length 2c, and operates at a frequency fc (usually the high pass cutoff frequency). The filter has a degree 2n-1 insertion function, therefore even though it only has n stubs, its highpass response contains 2n-1 ripples.

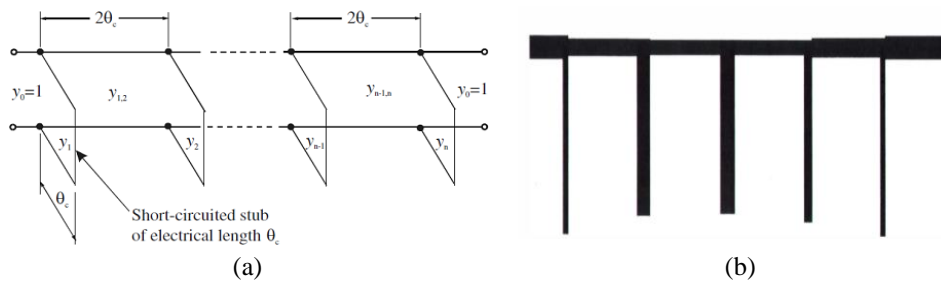(a)   (b)

Figure 1. Design of the distributed highpass filter (a) optimal distributed highpass filter and (b) fundamental design of optimum distributed highpass filter [1]

The (1) can be used to determine the electrical length θ_c as illustrated in Figure 1(a). Figure 1 shows the anticipated design of highpass filters with 2-6 stubs and a pass band ripple of 0.1 dB for $\theta_c = 25°$, $30°$ and $35°$. Figure 2 summarizes the parameters of the network. When Z_0 is the terminating impedance [1], the normalized characteristic admittance of transmission line components are tabulated, and the related characteristic line impedance are calculated using (2) and (3).

$$f = f_c \left(\pi/\theta_c - 1 \right) \tag{1}$$

$$Z_i = Z_0/y_i \tag{2}$$

$$Z_{i,\,+1} = Z_0/y_{i,\,+1} \tag{3}$$

n	θ_c	y_1 y_n	$y_{1,2}$ $y_{n-1,n}$	y_2 y_{n-1}	$y_{2,3}$ $y_{n-2,n-1}$	y_3 y_{n-2}	$y_{3,4}$
2	25°	0.15436	1.13482				
	30°	0.22070	1.11597				
	35°	0.30755	1.08967				
3	25°	0.19690	1.12075	0.18176			
	30°	0.28620	1.09220	0.30726			
	35°	0.40104	1.05378	0.48294			
4	25°	0.22441	1.11113	0.23732	1.10361		
	30°	0.32300	1.07842	0.39443	1.06488		
	35°	0.44670	1.03622	0.60527	1.01536		
5	25°	0.24068	1.10540	0.27110	1.09317	0.29659	
	30°	0.34252	1.07119	0.43985	1.05095	0.48284	
	35°	0.46895	1.02790	0.66089	0.99884	0.72424	
6	25°	0.25038	1.10199	0.29073	1.08725	0.33031	1.08302
	30°	0.35346	1.06720	0.46383	1.04395	0.52615	1.03794
	35°	0.48096	1.02354	0.68833	0.99126	0.77546	0.98381

Figure 2. Admittance value of microstrip high pass filters with 0.1 dB ripple [1]

2.2. Optimum bandstop filter

On specific frequencies, band pass filters are employed to block undesired transmissions. Figure 3 depict the transmission line network of a bandstop filter at the mid-stop-band frequency with open-circuited stubs. Figure 3(a) presents the bandstop filter with open-circuited stubs and Figure 3(b) presents the fundamental design of bandstop filter with open-circuited stub.
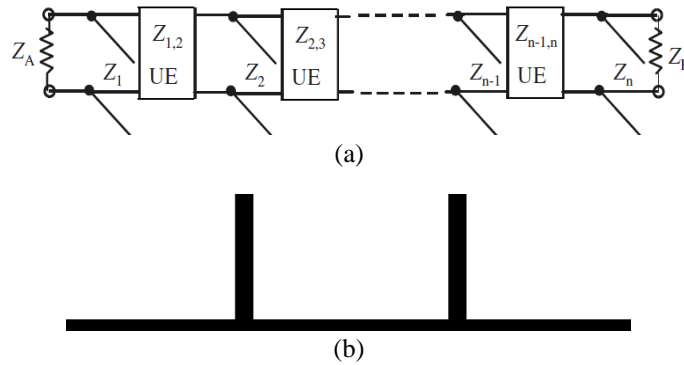

(a)

(b)

Figure 3. The transmission line network of a bandstop filter; (a) bandstop filter with open-circuited stubs and (b) fundamental design of bandstop filter with open-circuited stubs [1]

The open-circuited, quarter-wavelength stubs divide the shunt into unit elements with a length of one wavelength [1]. Figure 4 displays the specifications of the best bandstop filters for n=3. The two termination impedances, Z_A and Z_B, and the characteristic impedances, Z_i for open-circuited stubs and $Z_{i,i+1}$ for unit components, are what determine the filter's filtration capabilities [1].

$$Z_i = Z_0/g_i \tag{4}$$

$$Z_{i,+1} = Z_0/j_{i,+1} \tag{5}$$

FBW	$g_1 = g_3$	g_2	$J_{1,2} = J_{2,3}$
0.3	0.16318	0.26768	0.97734
0.4	0.23016	0.38061	0.92975
0.5	0.37754	0.63292	0.83956
0.6	0.46895	0.79494	0.78565
0.7	0.56896	0.97488	0.73139
0.8	0.67986	1.17702	0.67677
0.9	0.80477	1.40708	0.62180
1.0	0.94806	1.67311	0.56648
1.1	1.11601	1.98667	0.51082
1.2	1.15215	2.06604	0.49407
1.3	1.37952	2.49473	0.43430
1.4	1.67476	3.05136	0.37349
1.5	2.07059	3.79862	0.31262

Figure 4. Optimal bandstop filter element values for n=3 [1]

3. RESULTS AND DISCUSSION

3.1. Optimum distributed highpass filter

Figure 5 depicts the simulation of the highpass filter. The substrate used in the design, RO5880, has a dielectric constant of 2.2, a loss tangent of 0.0009, and a substrate height of 1.6 mm. The obtained graph after the simulation of highpass filter is shown in Figure 6. In the recommended work, the result is estimated in the frequency range of 0.1 to 4 GHz. Passband was considered up to 6 GHz for 0.1 dB ripple when developing such a microstrip highpass filter with a cutoff frequency of 1 GHz. Table 1 provides an overview of the widths and physical lengths of the stubs connected to the characteristic admittances of the microstrip line, which may be calculated using equations.
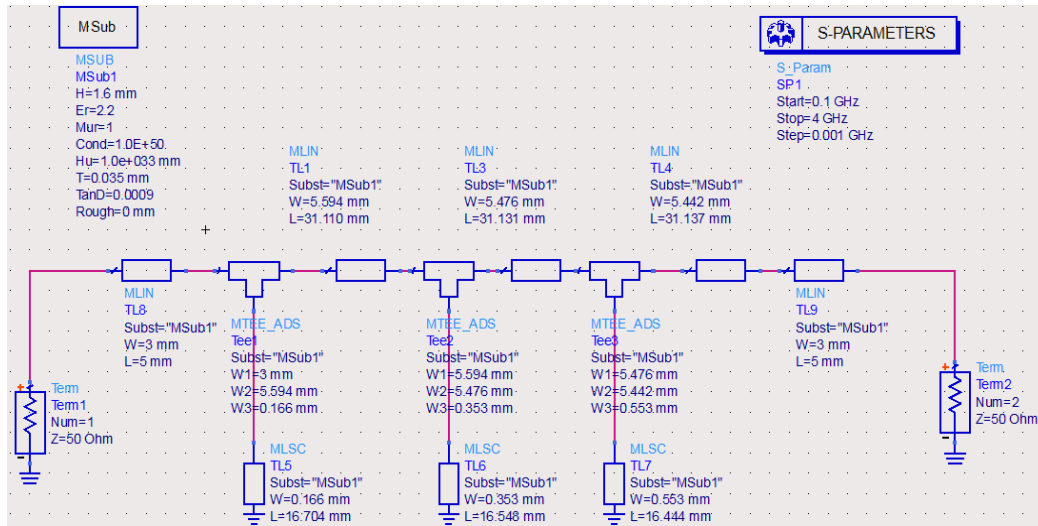
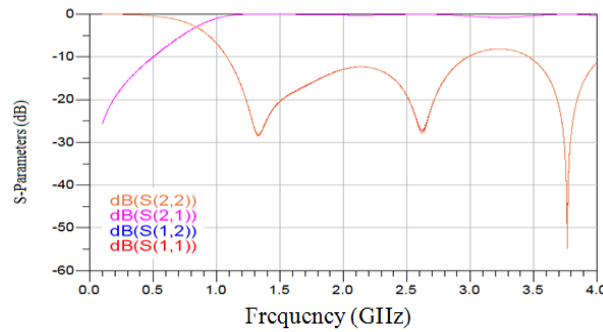Figure 5. Design of the proposed high pass filter

Figure 6. Graph of high pass filter

Table 1. Basic design parameters of microstrip high pass filter

y_i	Z_i (Ohm)	W_i (mm)	L_i (mm)
y_1=0.26501	Z_1=188.67	W_1=0.166	L_1=16.704
$y_{1,2}$=1.09704	$Z_{1,2}$=45.57	$W_{1,2}$=5.594	$L_{1,2}$=31.11
y_2=0.31531	Z_2=158.57	W_2=0.353	L_2=16.548
$y_{2,3}$=1.08110	$Z_{2,3}$=46.24	$W_{2,3}$=5.476	$L_{2,3}$=31.131
y_3=0.35811	Z_3=139.62	W_3= 0.553	L_3=16.444

The admittance values for θ_c=25.71° is calculated by interpolation from the admittance values shown in Table 1. Three short circuited stubs are included in the design of the microstrip highpass filter. The admittance values are selected for n=6 and θ_c=25° from Figure 2, which provides a good bandwidth up to 6 GHz, because the electrical length and the bandwidth are inversely proportional to each other. The admittance value y_1 is determined as follows for n=6 and θ_c=25.71°.

$$y_1=0.25038 + [(0.35346-0.25038)/5(25.71-25)]$$
$$y_1=0.26501$$

Similar information may be found in Table 1 for the remaining element values. The characteristic impedances for microstrip line elements are determined using (2)-(3). The microstrip high pass filter has a 50 Ω port at each end for supplying input signals and measuring output response. Figure 5 illustrates the basic nature of a microstrip filter, which consists of three quarter-wavelength stubs connected together by connecting microstrip lines. The cutoff frequency is indicated in Figure 6 as 1.1 GHz on the graph. Perfect impedance matching is implied by the return loss following the 1.48 GHz signal.

3.2. Optimum bandstop filter

The filter was designed using the ADS solver see Figure 7, where roger RO5880 is selected as a substrate with dielectric constant of 2.2, loss tangent 0.0009 and height of substrate 1.6 mm. For n =3 and by using (4) and (5) the characteristic impedances for the Microstrip line elements are calculated. All these impedance of transmission lines are sent by the 1st solver along with the substrate parameters. Table 2 displays this filter's dimensions. The simulation results of a band stop filter done using the ADS solver simulator see Figure 8 shows cutoff frequencies at f_1=1.4 GHz and f_2=3.45 GHz.
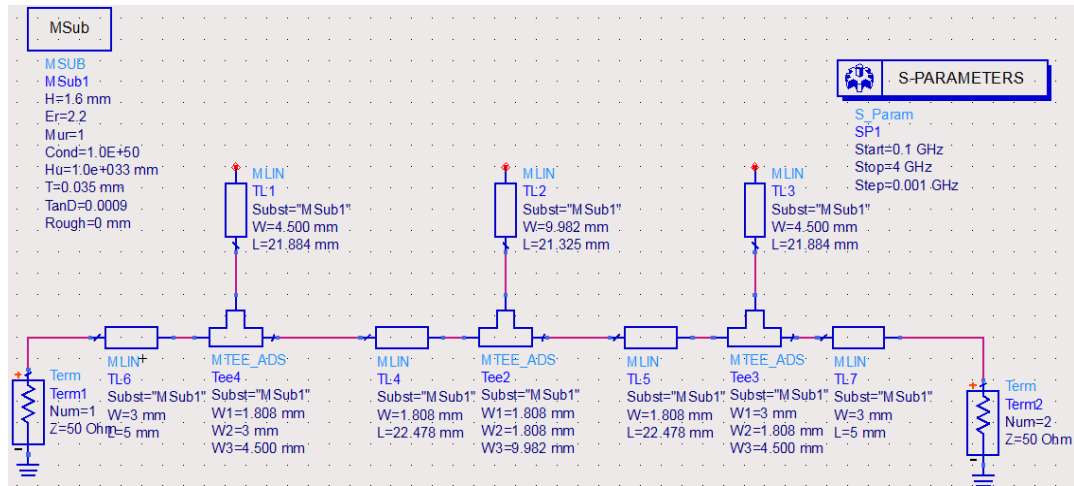

Figure 7. The band-stop filter circuit

Table 2. Dimensions of the bandstop filter

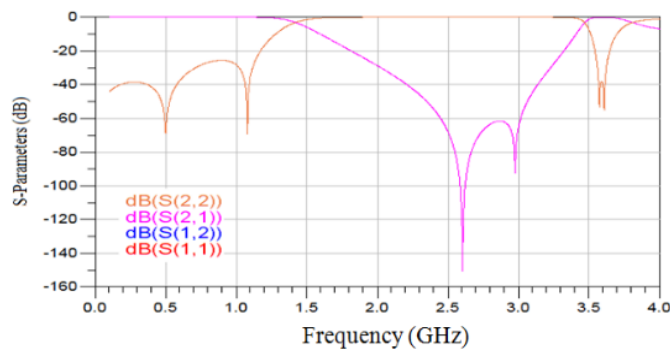| g_i/J_i	Z_i (Ohm)	W_i (mm)	L_i (mm)
g_1=g_3=0.94806	Z_1=Z_3= 52.74	L_1=L_3=21.884	W_1=W_3=4.50
g_2=1.67311	Z_2=29.88	L_2=21.325	W_2=9.982
$J_{1,2}$=$J_{2,3}$=0.56648	$Z_{1,2}$=$Z_{2,3}$=88.26	$L_{1,2}$=$L_{2,3}$=22.478	$W1,2$=$W_{2,3}$=1.808
g1= g3=0.94806	Z_1=Z_3= 52.74	L_1=L_3=21.884	W_1=W_3=4.500

Figure 8. S-parameter of the band stop filter

3.3. Dual bandpass filter

The high pass filter and band stop filter showed in Figure 9 are cascaded directly to form a dual band pass filter. In this circuit, three shorted stubs are used. The dielectric material used as a substrate is RO5880 substrate which has thickness of 1.6 mm, loss tangent of 0.0009 and dielectric constant of 2.2. The whole area of the proposed circuit is 60×178,3 mm^2. Tables 3 and 4 list different values of the short-circuited shunts of sections of electrical length c and connection lines of electrical length 2c. After the comparison of the results obtained through the parametric studies carried out (Figures 10 and 11) and as illustrated in Figure 12, the simulated central frequencies are 1.19 and 3.50 GHz.
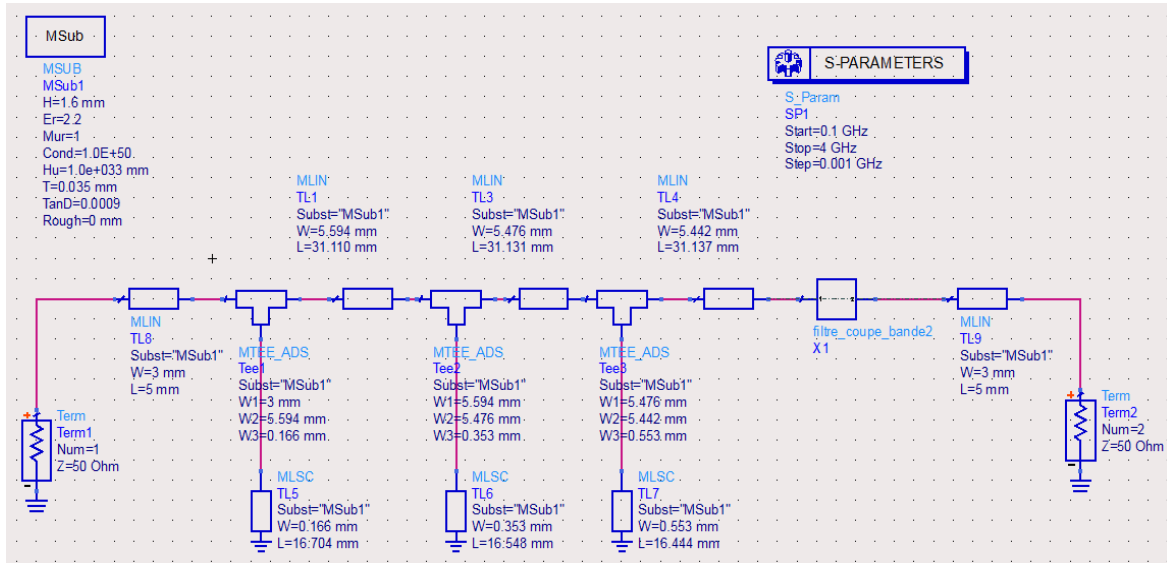
Figure 9. Geometry of the dual band pass filter

Table 3. The different values of the parameter 'w' of electrical length c

Parameter	Value 1	Value 2	Value 3
W_1	2.594	5.594	8.594
W_2	2.476	5.476	8.476
W_3	2.442	5.442	8.442

Table 4. The different values of the parameter 'w' of electrical length 2c

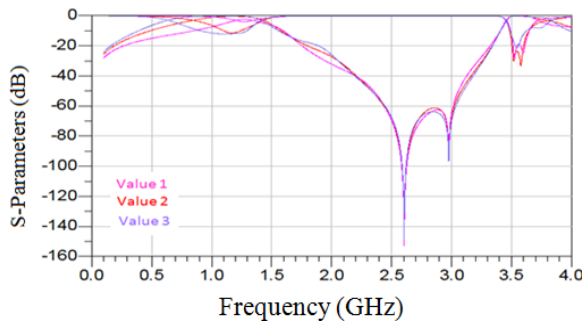| Parameter	Value 1	Value 2	Value 3
W_1	0.166	2.166	4.166
W_2	0.353	2.353	4.353
W_3	0.553	2.553	4.553

Figure 10. Simulation results for the suggested filter for different electrical length c values, indicated by "w"
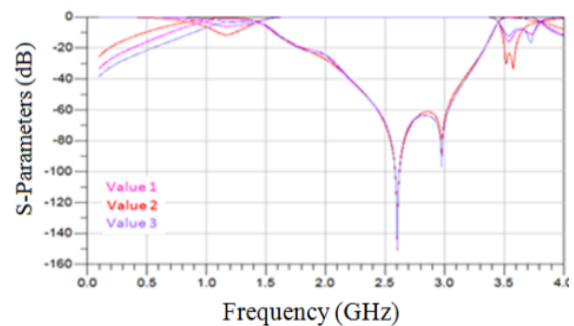

Figure 11. Simulation results of proposed filter versus the value of 'w' of electrical length 2c
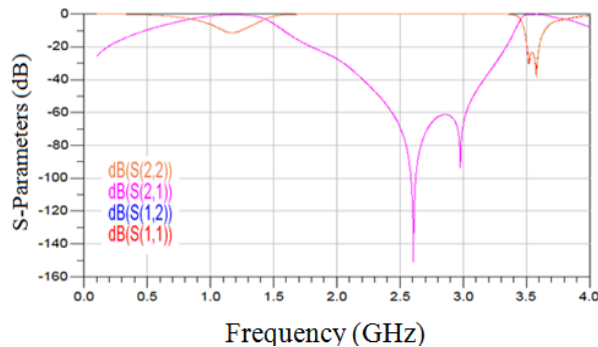

Figure 12. Results of simulation using moments method for the suggested dual band pass filter

A deep transmission zero between the two bands was located at 2.6 GHz, resulting in high isolation with an attenuation level of more than -150 dB. The return losses of the first and second bands (at the central frequencies) are 13 dB and 40 dB and insertion losses of them are 0.37 dB and 0.24 dB. We repeated the analysis using a different electromagnetic solver using finite integration technique (FIT) from CST which is 3D design to confirm the simulation results obtained with the first solver by using moments method, Table 5 shows all dimension parameters as shown in Figure 13. Figure 14 show the perspective view of the 3D layout of the suggested dual bandpass filter using FIT. As illustrated in Figure 15, and compared with Figure 12 we have a dual band pass filter behavior with a minor variance due to the various numerical techniques utilized in these electromagnetic solvers.

Table 5. The suggested filter's optimized dimensions

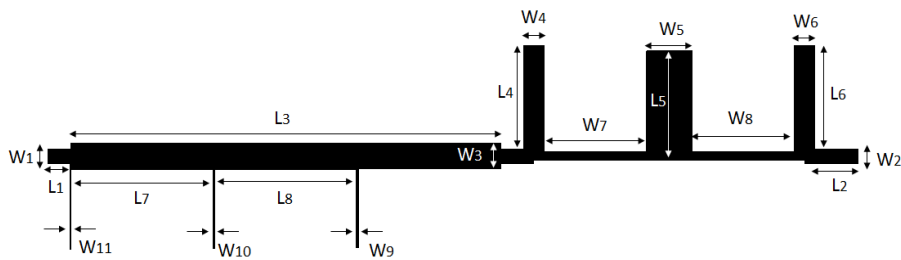| Parameter	Value	Parameter	Value
W_1	3	W_6	4.5
L_1	5.083	L_6	21.884
W_2	3	W_7	22.478
L_2	12.25	L_7	31.11
W_3	5.442	W_8	22.478
L_3	94.367	L_8	31.131
W_4	4.5	W_9	0.553
L_4	22.48	W_{10}	0.353
W_5	9.982	W_{11}	0.166
L_5	31.325		

Figure 13. The dual band-pass filter comparable circuit created by the second solver
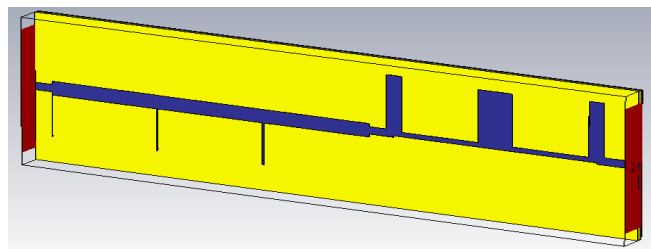

Figure 14. Three-dimensional depiction of the proposed filter
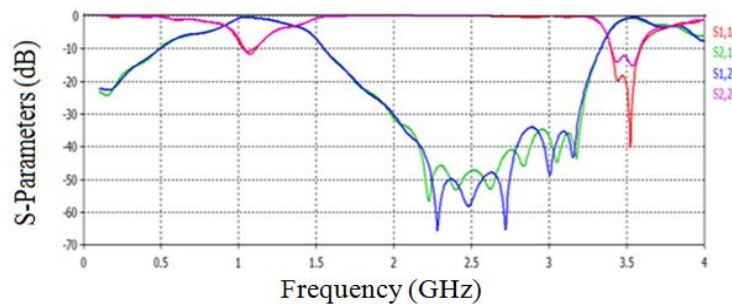

Figure 15. Simulation results of proposed band pass filter by FIT

Figure 16 presents the current distributions of the proposed filter for frequencies of 1.19 GHz, 2.5 GHz, and 3.5 GHz. This demonstrates that the current is effectively transmitted from the input to the output terminal for the bandpass frequencies at 1.19 GHz and 3.5 GHz. At 2.5 GHz the signal is largely attenuated from reaching the output. The comparison between our study and the literatures is shown in Table 6, which concludes that the recommended filter performs well compared to other filters in terms of S_{11}, which is very high at 3.5 GHz, as well as for S_{21} which has good attenuation.
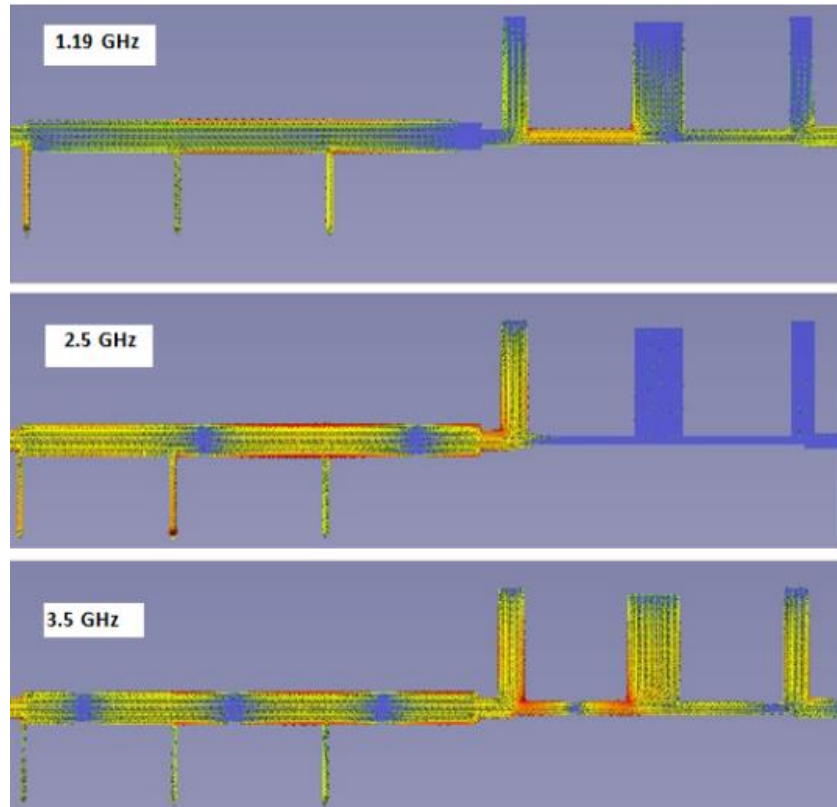

Figure 16. The suggested filter's current distribution at various frequencies

Table 6. Comparison of the proposed filter and others structures

Ref	Bands (GHz)	S_{21} (dB)	S_{11} (dB)	FBW (%)
[19]	0.85	0.98	15	16.84
[20]	0.98	0.9	17	20
[21]	3.5	1.3	28.6	6.23
[22]	3.4	0.37	19	12
This work	1.19/3.5	0.24/0.37	13/40	39.5/11.14

4. CONCLUSION

For mobile phone and WiMAX applications, a novel dual bandpass microstrip filter with outstanding electrical performance and compact size is proposed. It consists of a stop band filter and a high-pass filter. The dual bandpass filter consists of two operating frequency bands, one around 1.19 GHz and the second one at 3.50 GHz. The RO5880 substrate is used to mount the recommended filter. Because this study is theoretical in nature and may be tailored to appropriate frequency bands, It is compatible with more frequency bands. Using two distinct electromagnetic simulators, we examined the suggested circuit's frequency response. Furthermore, the final recommended circuit operates effectively in terms of insertion loss and return loss. Among perspectives of this study, the recommended filter can be associated to active components as varactors permitting to control and to adjust the frequency band making the proposed filter reconfigurable in term of frequency band.

REFERENCES

[1]   J. Hong and M. J. Lancaster, "Microstrip filters for RF/Microwave," vol. 7, pp. 0–471, 2001.
[2]   C. W. Tang, C. H. Yang, and J. S. Liao, "Design of planar wide-stopband bandstop filters with extra-high attenuation," *IEEE Transactions on Circuits and Systems II: Express Briefs*, vol. 69, no. 3, pp. 1039–1043, 2022, doi: 10.1109/TCSII.2021.3137667.
[3]   N. Mittal and M. K. Pandey, "Design of microstrip high pass filter using optimum distributed technique for GSM applications," *International Journal of Computer Sciences and Engineering*, vol. 6, no. 7, pp. 1555–1558, Jul. 2018, doi: 10.26438/ijcse/v6i7.15551558.
[4]   R. Ahmed, S. Emiri, and S. T. Imeci, "Design and analysis of a bandpass hairpin filter," in *2018 International Applied Computational Electromagnetics Society Symposium in Denver, ACES-Denver 2018*, Mar. 2018, pp. 1–2, doi: 10.23919/ROPACES.2018.8364310.
[5]   M. Mabrok, Z. Zakaria, Y. E. Masrukin, T. Sutikno, A. R. Othman, and N. Edward, "Switchable dual-band bandpass filter based on stepped impedance resonator with U-shaped defected microstrip structure for wireless applications," *Telkomnika (Telecommunication Computing Electronics and Control)*, vol. 17, no. 2, pp. 1032–1039, Apr. 2019, doi: 10.12928/TELKOMNIKA.V17I2.11637.
[6]   N. Wang *et al.*, "Dual-band bandpass filter with controllable stopband bandwidth," *Frontiers in Physics*, vol. 9, Jan. 2022, doi: 10.3389/fphy.2021.809752.
[7]   Z. Troudi, J. Machac, and L. Osman, "Miniaturised planar band-pass filter based on interdigital arm SRR," *IET Microwaves, Antennas and Propagation*, vol. 13, no. 12, pp. 2081–2086, Oct. 2019, doi: 10.1049/iet-map.2018.5708.
[8]   S. B. Haddi, A. Zugari, A. Zakriti, and S. Achraou, "Design of a band-stop planar filter for telecommunications applications," *Procedia Manufacturing*, vol. 46, pp. 788–792, 2020, doi: 10.1016/j.promfg.2020.04.006.
[9]   S. Seghier, N. Benabdallah, N. Benahmed, and K. Nouri, "Design and optimization of a microstrip bandpass filter for ultra wideband (UWB) wireless communication," *International Journal of Information and Electronics Engineering*, vol. 6, no. 4, p. 230, 2016, doi: 10.18178/IJIEE.2016.6.4.630.
[10]   S. F. Abdulkareem, Z. Faydh, and D. H. Al-Nuaimi, "Investigation of dualband fan-shaped microstrip bandpass filter," *Telkomnika (Telecommunication Computing Electronics and Control)*, vol. 19, no. 1, pp. 229–234, Feb. 2021, doi: 10.12928/TELKOMNIKA.V19I1.16507.
[11]   H. Lu, J. Huang, X. Zhang, N. Yuan, and Z. Huang, "Dual-mode dual-band microstrip bandpass filter based on stepped impedance resonator (SIR) for wireless communication applications," 2017, doi: 10.2991/ceie-16.2017.98.
[12]   B. Nasiri, A. Ennajih, A. Errkik, J. Zbitou, and M. Derri, "Band-pass filter based on complementary split ring resonator," *Telkomnika (Telecommunication Computing Electronics and Control)*, vol. 18, no. 3, pp. 1145–1149, Jun. 2020, doi: 10.12928/TELKOMNIKA.v18i3.13929.
[13]   A. Belmajdoub, M. Jorio, S. Bennani, A. Lakhssassi, and M. Amzi, "Design of compact microstrip bandpass filter using square DMS slots for Wi-Fi and bluetooth applications," *Telkomnika (Telecommunication Computing Electronics and Control)*, vol. 19, no. 3, pp. 724–729, Jun. 2021, doi: 10.12928/TELKOMNIKA.v19i3.18768.
[14]   A. Boutejdar, M. Amzi, and S. D. Bennani, "Design and improvement of a compact bandpass filter using DGS technique for WLAN and WiMAX applications," *Telkomnika (Telecommunication Computing Electronics and Control)*, vol. 15, no. 3, pp. 1137–1144, Sep. 2017, doi: 10.12928/TELKOMNIKA.v15i3.6917.
[15]   E. Sghir, A. Errkik, J. Zbitou, L. El Abdellaoui, A. Tajmouati, and M. Latrach, "A novel compact CPW tunable stop band filter using a new Z-DGS-resonator for microwave applications," *Telkomnika (Telecommunication Computing Electronics and Control)*, vol. 17, no. 5, pp. 2410–2417, Oct. 2019, doi: 10.12928/TELKOMNIKA.v17i5.12193.
[16]   A. Kadiri, A. Tajmouati, J. Zbitou, I. Zahraoui, and M. Latrach, "Design of a compact and miniature band-pass filter for global positioning system applications," *Indonesian Journal of Electrical Engineering and Computer Science*, vol. 26, no. 3, pp. 1274–1280, 2022, doi: 10.11591/ijeecs.v26.i3.pp1274-1280.
[17]   A. Kadiri, A. Tajmouati, I. Zahraoui, A. R. A. Laaraibi, and M. Latrach, "A planar high pass filter with quasilumped elements for ISM, Wimax and wlan applications," in *2020 IEEE 2nd International Conference on Electronics, Control, Optimization and Computer Science, ICECOCS 2020*, Dec. 2020, pp. 1–4, doi: 10.1109/ICECOCS50124.2020.9314620.
[18]   A. Kadiri, A. Tajmouati, J. Zbitou, I. Zahraoui, A. Errkik, and M. Latrach, "A new design of a miniature microstrip bandpass filter for DCS applications," *E3S Web of Conferences*, vol. 351, p. 01083, May 2022, doi: 10.1051/e3sconf/202235101083.
[19]   A. Basit, M. I. Khattak, A. R. Sebak, A. B. Qazi, and A. A. Telba, "Design of a compact microstrip triple independently controlled pass bands filter for GSM, GPS and WiFi applications," *IEEE Access*, vol. 8, pp. 77156–77163, 2020, doi: 10.1109/ACCESS.2020.2989377.
[20]   M. U. Rahman, D. S. Ko, and J. D. Park, "A compact tri-band bandpass filter utilizing double mode resonator with 6 transmission zeros," *Microwave and Optical Technology Letters*, vol. 60, no. 7, pp. 1767–1771, Jul. 2018, doi: 10.1002/mop.31239.
[21]   R. C. Caleffo and F. S. Correra, "A novel and compact 3.5 GHz tunable bandpass filter in SIW technology with shunt-inductive discontinuities switched by pin diode switches," *Microwave and Optical Technology Letters*, vol. 63, no. 2, pp. 471–479, Feb. 2021, doi: 10.1002/mop.32640.
[22]   T. A. Sheikh, J. Borah, and S. Roy, "Design of compact bandpass filter for WiMAX and UWB application using asymmetric SIRs and DGS," *Radioelectronics and Communications Systems*, vol. 59, no. 6, pp. 269–273, Jun. 2016, doi: 10.3103/S0735272716060066.
[23]   D. Tang, C. Han, Z. Deng, H. J. Qian, and X. Luo, "Compact bandpass filter with wide stopband and low radiation loss using substrate integrated defected ground structure," in *IEEE MTT-S International Microwave Symposium Digest*, Aug. 2020, vol. 2020-August, pp. 671–674, doi: 10.1109/IMS30576.2020.9224103.
[24]   J. Xu, K. Da Xu, M. Zhang, and Q. Chen, "Dual-band bandpass filter using two simple coupled microstrip rings," *Engineering Reports*, vol. 3, no. 2, Feb. 2021, doi: 10.1002/eng2.12288.
[25]   A. Lalbakhsh *et al.*, "A design of a dual-band bandpass filter based on modal analysis for modern communication systems," *Electronics (Switzerland)*, vol. 9, no. 11, pp. 1–13, Oct. 2020, doi: 10.3390/electronics9111770.
[26]   M. Sazid and N. S. Raghava, "Planar UWB-bandpass filter with multiple passband transmission zeros," *AEU - International Journal of Electronics and Communications*, vol. 134, p. 153711, May 2021, doi: 10.1016/j.aeue.2021.153711.

BIOGRAPHIES OF AUTHORS

Amal Kadiri [iD] [SC] was born in Berrechid, Morocco, on November in 1983. She received a Master's degree in Telecommunication from the Faculty of Sciences of Settat, Hassan First University, Morocco, in 2009. Currently, she is a Ph.D. student in Sciences at the Faculty of Sciences and Techniques of Settat, Hassan First University, Morocco. Her current research interests are around the study and design of planar microstrip filters. She can be contacted at email: a.kadiri@uhp.ac.ma.

Abdelali Tajmouati [iD] [SC] was born in Morocco in 1962. He is Senior member of IEEE; he received a Ph.D. degree in science engineering from the University of Perpignan, France, in 1992. He is currently a full Professor of Electronics, thermal transfer, and thermodynamic at the Faculty of Sciences and Techniques of Settat, Hassan First University, Morocco. He is involved in the design of the hybrid, monolithic, active, and passive microwave electronic circuits. He can be contacted at email: tajmoua@gmail.com.

Jamal Zbitou [iD] [SC] was born in Fes, Morocco, in June 1976. He is Senior member of IEEE; he received a Ph.D. degree in electronics from Polytech of Nantes, the University of Nantes, France, in 2005. Currently He is a full Professor of Electronics at ENSA of Tetouan Morocco. He is involved in the design of the hybrid, monolithic, active, and passive microwave electronic circuits. He can be contacted at email: j.zbitou@uae.ac.ma.

Ahmed Lakhssassi [iD] [SC] is senior member of IEEE; he received the B.Eng. and M.Sc. A in electrical engineering from University of Québec à Trois-Rivières (UQTR), Québec, Canada in 1988 and 1990 respectively. He also received the Ph.D. in Energy and Material sciences in 1995 from INRS-Energy et Materia (National Institute for Scientific Research), Québec, Canada. Since 1998, he has been with UQO (University of Québec - Outaouais), where he is currently titular professor and responsible of the LIMA laboratory (advanced microsystem engineering laboratory). He can be contacted at email: ahmed.lakhssassi@uqo.ca.